

Sharp Phase Boundary for Quantum Reverse Diffusion

Ammar Fayad¹

¹*Massachusetts Institute of Technology, Cambridge, Massachusetts 02139, USA*

Classical reverse diffusion is generated by changing the drift at fixed noise. We show that the quantum version of this principle obeys an exact law with a sharp phase boundary. For Gaussian pure-loss dynamics, the canonical model of continuous-variable decoherence, we prove that the unrestricted instantaneous reverse optimum exhibits a noiseless-to-noisy transition: below a critical squeezing-to-thermal ratio, reversal can be noiseless; above it, complete positivity forces irreducible reverse noise whose minimum cost we determine in closed form. The optimal reverse diffusion is uniquely covariance-aligned and simultaneously minimizes the geometric, metrological, and thermodynamic price of reversal. For multimode trajectories, the exact cost is additive in a canonical set of mode-resolved data, and a globally continuous protocol attains this optimum on every mixed-state interval. If a pure nonclassical endpoint is included, the same pointwise law holds for every $t > 0$, but the optimum diverges as $2/t$: exact Gaussian reversal of a pure quantum state is dynamically unattainable. These results establish the exact Gaussian benchmark against which any broader theory of quantum reverse diffusion must be measured.

Reversing an irreversible process without paying extra noise is one of the deepest idealizations behind classical diffusion theory [1, 2]. In modern score-based language, reverse diffusion is generated by changing the drift while keeping the noise level fixed [3–6]. Recent work has made the quantum version of this problem newly urgent by identifying a semiclassical bridge between Bayes reverse diffusion and quantum reversibility via the Petz map [12–15]. The natural question is whether quantum reverse dynamics obeys a comparably sharp law, or whether the extra constraints of quantum mechanics destroy any clean analogue of classical reversibility.

We show that the answer is an exact law with three surprising features. First, the unrestricted quantum reverse optimum exhibits a sharp phase boundary: below a critical squeezing-to-thermal ratio, reversal is completely noiseless; above it, quantum mechanics forces irreducible reverse noise whose minimum cost we determine in closed form. Second, the optimal reverse protocol simultaneously minimizes three independently motivated physical quantities—the displacement quantum Fisher-information injection rate, the displacement-Bures rate, and the fluctuation entropy production—so the boundary at which reversal becomes free is the point at which geometric, metrological, and thermodynamic costs all vanish together. Third, pure nonclassical states are singular: the exact pointwise optimum diverges universally as $2/t$, so no finite continuous protocol can reach a pure quantum endpoint. Exact reversal of a pure nonclassical state is dynamically unattainable.

These results hold for Gaussian pure-loss dynamics—the canonical model of continuous-variable decoherence [7–9]—and are proved within the class of Gaussian Markov generators. The basic obstruction is generator-level complete positivity [9, 10]. A Gaussian Markov generator (K_t, D_t) evolves the covariance matrix Γ_t by

$$\dot{\Gamma}_t = K_t \Gamma_t + \Gamma_t K_t^T + D_t, \quad (1)$$

and complete positivity requires

$$D_t + i(K_t \sigma + \sigma K_t^T) \succeq 0. \quad (2)$$

Drift and diffusion are therefore coupled at the generator level: the classical reverse-by-drift picture cannot simply be transplanted into quantum dynamics [9–11].

For one mode, the forward pure-loss dynamics is

$$K_{\text{fwd}} = -\gamma I_2, \quad D_{\text{fwd}} = 2\gamma I_2, \quad (3)$$

with covariance path

$$\Gamma_t = e^{-2\gamma t} \Gamma_0 + (1 - e^{-2\gamma t}) I_2. \quad (4)$$

For a squeezed-thermal target

$$\Gamma_0 = \text{diag}(\nu e^{2r}, \nu e^{-2r}), \quad (5)$$

one can construct a fixed-diffusion Bayes reverse candidate that keeps the forward noise and modifies only the drift. This candidate is completely positive if and only if $\cosh(2r) \leq \nu$. Our first main result is that this boundary is not an artifact of the Bayes ansatz: it is the exact noiseless transition of the unrestricted instantaneous Gaussian reverse problem. Below it, the global optimum achieves zero reverse noise. Above it, every admissible Gaussian reverse generator must inject strictly positive diffusion.

The cost functional that the optimum minimizes,

$$Z(D; \Gamma) := \text{Tr}(\Gamma^{-1} D), \quad (6)$$

is the natural reverse-diffusion budget: it simultaneously measures the displacement-SLD quantum Fisher-information injection rate, four times the displacement-Bures rate, and the fluctuation contribution to the Gaussian de Bruijn entropy-production law [16, 17]. This triple coincidence means that the same boundary and the same optimizer govern the geometric, metrological, and thermodynamic price of reversal.

The one-mode law admits a full multimode completion. For multimode pure-loss trajectories, the exact reverse cost remains additive in a canonical set of mode-resolved anti-squeezing data, and this additive law is the exact unrestricted Gaussian optimum on every interval for which all symplectic eigenvalues remain strictly above one. Crossings and degeneracies do not destroy exactness: a globally continuous moving Williamson frame reduces the multimode problem to independent scalar mode optimizations. If a pure nonclassical endpoint is included, the same pointwise law holds for every $t > 0$, but the optimum diverges universally as $2/t$. Exact Gaussian reversal of a pure nonclassical target is therefore dynamically unattainable.

The result is relevant beyond Gaussian channel theory. Reverse-diffusion constructions are now discussed in quantum settings partly through the Bayes–Petz correspondence [12–15], and our law identifies the exact benchmark governing when such constructions can remain noiseless and when irreducible reverse noise is unavoidable. As a concrete scale, direct optical squeezing at the 15 dB level corresponds to $\cosh(2r) \approx 15.8$ [18], so noiseless Gaussian reverse dynamics at that squeezing level would require $\nu \geq 15.8$. Otherwise the unrestricted instantaneous Gaussian optimum must inject reverse diffusion.

For Gaussian pure-loss dynamics, reversibility is separated by an exact boundary: below $\cosh(2r) = \nu$ reversal can be noiseless, above it irreducible reverse noise is unavoidable, and the pure nonclassical boundary is singular.

Bayes reverse threshold.— For the one-mode pure-loss channel, the fixed-diffusion Bayes reverse candidate keeps the forward diffusion and modifies only the drift,

$$K^{\text{Bayes}} = K_{\text{fwd}} + D_{\text{fwd}}\Gamma_0^{-1}, \quad D^{\text{Bayes}} = D_{\text{fwd}}. \quad (7)$$

Its complete-positivity matrix is

$$M^{\text{Bayes}} = D^{\text{Bayes}} + i(K^{\text{Bayes}}\sigma + \sigma(K^{\text{Bayes}})^T). \quad (8)$$

For the $i\sigma$ -eigenvector $u = \frac{1}{\sqrt{2}}(1, i)^T$, one finds

$$u^\dagger M^{\text{Bayes}} u = 4\gamma \left(1 - \frac{\cosh(2r)}{\nu} \right). \quad (9)$$

Hence the fixed-diffusion Bayes reverse lift is completely positive if and only if

$$\cosh(2r) \leq \nu. \quad (10)$$

Figure 1 shows the resulting phase boundary. Beyond it, the direct classical reverse-drift prescription becomes unphysical, and a strictly positive reverse cost turns on.

Exact instantaneous one-mode optimum.— We now solve the unrestricted instantaneous reverse problem. Among all one-mode Gaussian generators (K, D) satisfying exact reverse covariance matching at Γ_0 and

generator complete positivity, we minimize $Z(D; \Gamma_0)$. Writing

$$x := \frac{\cosh(2r)}{\nu}, \quad (11)$$

the exact optimum is

$$Z_{\min} = \frac{4\gamma|x-1|}{\nu - \text{sgn}(x-1)}. \quad (12)$$

Equivalently,

$$x < 1 \Rightarrow Z_{\min} = \frac{4\gamma(1-x)}{\nu+1}, \quad x > 1 \Rightarrow Z_{\min} = \frac{4\gamma(x-1)}{\nu-1}. \quad (13)$$

Moreover, the unique optimal diffusion tensor is covariance-aligned,

$$D_{\text{opt}} = \frac{Z_{\min}}{2}\Gamma_0. \quad (14)$$

Thus the fixed-diffusion threshold survives as the exact noiseless transition of the unrestricted Gaussian reverse problem:

$$Z_{\min} = 0 \iff \cosh(2r) = \nu. \quad (15)$$

The derivation is structurally rigid: exact rank-one dual witnesses certify the optimum, and complementary slackness forces covariance alignment rather than assuming it. The boundary at $\cosh(2r) = \nu$ is therefore not a property of one failed reverse ansatz; it is the exact transition of the unrestricted instantaneous Gaussian optimum.

Physical currency of reverse diffusion.— The cost $Z(D; \Gamma)$ is the physically natural reverse budget. For faithful one-mode targets it is exactly the displacement-SLD quantum Fisher-information injection rate; equivalently, it is four times the displacement-Bures rate and

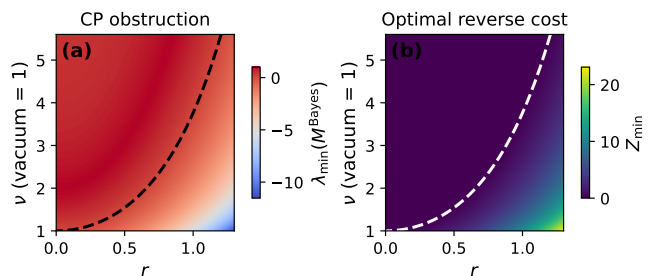


FIG. 1. Sharp phase boundary for Gaussian quantum reversibility under pure loss. (a) Minimum eigenvalue of the fixed-diffusion Bayes reverse CP matrix M^{Bayes} versus squeezing r and thermal variance ν (vacuum = 1). The dashed curve is the exact threshold $\nu = \cosh(2r)$. (b) Exact optimal reverse cost Z_{\min} for the unrestricted instantaneous one-mode Gaussian reverse problem. The same dashed curve marks the noiseless transition: below it $Z_{\min} = 0$, while above it irreducible reverse diffusion is forced by complete positivity.

proportional to the fluctuation contribution in the Gaussian de Bruijn entropy-production law [16, 17]. The same optimizer therefore minimizes geometric, metrological, and thermodynamic reverse fuel simultaneously. At the threshold $\cosh(2r) = \nu$, all three vanish together.

Multimode exact law.— For multimode pure-loss trajectories, the reverse cost obeys a gauge-invariant additive lower bound

$$Z(D_t; \Gamma_t) \geq \sum_k \frac{4\gamma |x_k^*(t) - 1|}{\nu_k(t) - \text{sgn}(x_k^*(t) - 1)}. \quad (16)$$

Here $x_k^*(t)$ are the canonical anti-squeezing data defined by the moving Williamson frame introduced below. Equation (16) says that dangerous modes contribute additively: neither spectator modes nor intermode structure can hide the reverse cost.

The lower bound is also exact. The multimode pure-loss path admits a globally continuous moving Williamson frame

$$\Gamma_t = S_c(t)\Lambda_t S_c(t)^T, \quad \Lambda_t = \bigoplus_{k=1}^N \nu_k(t) I_2, \quad (17)$$

for which the reverse problem obeys a simple source equation. Defining

$$W_c := S_c^{-1} \dot{S}_c, \quad G_t := S_c^{-1} S_c^{-T}, \quad (18)$$

one finds

$$R_t := -\dot{\Lambda}_t = 2\gamma(\Lambda_t - G_t) + W_c \Lambda_t + \Lambda_t W_c^T. \quad (19)$$

In the complex canonical representation this becomes

$$R_t^C = 2\gamma(\Lambda_t^C - G_t^C) + [W_t^C, \Lambda_t^C]. \quad (20)$$

Its off-diagonal entries give

$$(\nu_k - \nu_j) W_{t,jk}^C = 2\gamma G_{t,jk}^C, \quad j \neq k, \quad (21)$$

while the diagonal entries give the exact scalar reverse sources

$$s_k(t) = 2\gamma \nu_k(t) (1 - x_k^*(t)). \quad (22)$$

Crossings therefore cease to be singular, and the multimode problem reduces to independent one-mode scalar optimizations. The lower bound in Eq. (16) is attained by a globally continuous Gaussian CP reverse protocol, giving the exact unrestricted Gaussian optimum on every mixed-state interval.

Pure-endpoint singularity.— If a pure nonclassical endpoint is included, the same pointwise law remains valid for every $t > 0$, but the optimum diverges universally as

$$Z_{\min}(t) = \frac{2}{t} + O(1), \quad t \rightarrow 0^+. \quad (23)$$

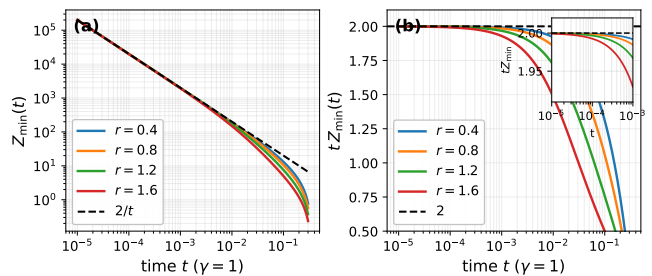


FIG. 2. Pure-endpoint singularity of the exact Gaussian reversibility law. For pure squeezed targets, the exact pointwise Gaussian reverse optimum diverges as $Z_{\min}(t) \sim 2/t$ as $t \rightarrow 0^+$. (a) The optimal cost approaches the universal asymptote $2/t$. (b) The rescaled quantity $tZ_{\min}(t)$ collapses to the universal coefficient 2, independent of the squeezing parameter r .

Figure 2 shows this thermodynamic unattainability: the pointwise optimum approaches the universal asymptote $2/t$, while the rescaled quantity $tZ_{\min}(t)$ collapses to the universal coefficient 2, independent of squeezing.

Discussion.— We have derived an exact law of Gaussian quantum reversibility for pure-loss dynamics. The unrestricted instantaneous optimum has a sharp noise-

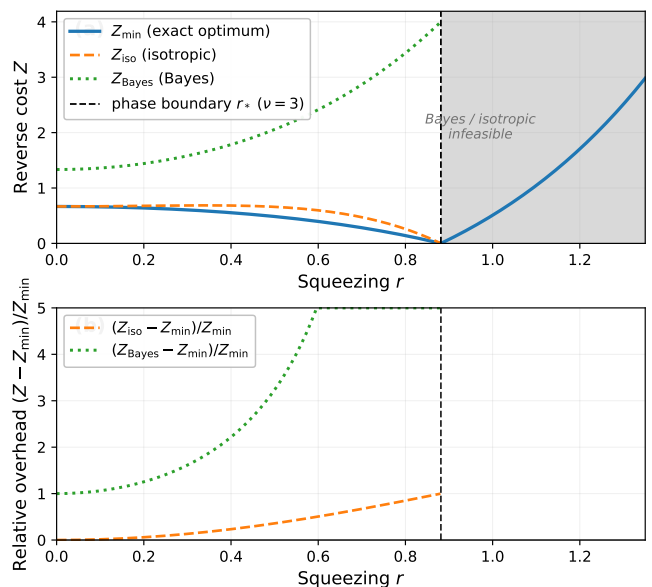


FIG. 3. Reverse-fuel cost of named Gaussian reverse protocols for a one-mode squeezed-thermal target under pure loss. The solid curve shows the exact optimum Z_{\min} , the dashed curve the best isotropic exact-reverse protocol with $D = cI_2$, and the dotted curve the fixed-diffusion Bayes reverse. The vertical dashed line marks the exact phase boundary $\cosh(2r) = \nu$ (here $\nu = 3$). Below threshold, naive protocols pay a strict reverse-fuel penalty relative to the covariance-aligned optimum; above threshold, both Bayes and isotropic protocols are infeasible, while the exact optimum remains feasible.

less transition at $\cosh(2r) = \nu$, the multimode optimum is exactly additive on every mixed-state interval, and pure nonclassical endpoints are singular. The same cost functional controls the geometric, metrological, and thermodynamic fuel required for reversal, so the law is not merely algebraic: it identifies the exact price of reversing an irreversible quantum process within the continuous Gaussian Markovian class.

The result also supplies an exact benchmark for reverse-diffusion constructions motivated by the Bayes–Petz correspondence [12–15]. It shows that in the canonical pure-loss setting, a classical reverse-drift picture does not simply fail heuristically; it is replaced by a sharp reversibility law with an exact optimizer and a singular pure boundary. For current optical platforms operating near 15 dB of squeezing, the noiseless threshold requires thermal variance $\nu \geq 15.8$ [18]; any attempt to reverse pure-loss decoherence of a state at or beyond that squeezing scale must inject irreducible noise whose minimum cost is fixed by the law derived here. Figure 3 compares the exact optimum against the fixed-diffusion Bayes reverse and the best isotropic reverse protocol for a squeezed-thermal state with $\nu = 3$. Both suboptimal protocols incur diverging overhead near the phase boundary and become infeasible above it, while the exact covariance-aligned optimum remains well defined throughout. For highly nonclassical bosonic targets, the pure-endpoint divergence identifies an intrinsic obstruction to exact Gaussian reversal that precedes any specific decoder architecture. For quantum diffusion models aiming to prepare or denoise continuous-variable states, the law says that learning a reverse drift alone cannot succeed: complete positivity enforces an exact reverse-noise budget and a singular pure-state boundary already in the canonical setting.

The broader open problem remains whether unrestricted non-Gaussian reverse protocols obey the same law, evade it, or realize a different optimum [19–21]. The present work does not answer that question. It fixes the exact Gaussian benchmark against which any broader theory of quantum reverse diffusion must now be measured.

[1] B. D. O. Anderson, Reverse-time diffusion equation models, *Stochastic Processes and their Applications* **12**, 313 (1982).
 [2] U. G. Haussmann and E. Pardoux, Time Reversal of Diffusions, *The Annals of Probability* **14**, 1188 (1986).
 [3] J. Sohl-Dickstein, E. Weiss, N. Maheswaranathan, and S. Ganguli, Deep Unsupervised Learning Using Nonequilibrium Thermodynamics, in *Proceedings of the 32nd International Conference on Machine Learning*, Proceedings

of Machine Learning Research **37**, 2256 (2015).
 [4] Y. Song and S. Ermon, Generative Modeling by Estimating Gradients of the Data Distribution, in *Advances in Neural Information Processing Systems* **32**, 11918 (2019).
 [5] J. Ho, A. Jain, and P. Abbeel, Denoising Diffusion Probabilistic Models, in *Advances in Neural Information Processing Systems* **33**, 6840 (2020).
 [6] Y. Song, J. Sohl-Dickstein, D. P. Kingma, A. Kumar, S. Ermon, and B. Poole, Score-Based Generative Modeling through Stochastic Differential Equations, in *International Conference on Learning Representations* (2021).
 [7] S. L. Braunstein and P. van Loock, Quantum information with continuous variables, *Reviews of Modern Physics* **77**, 513 (2005).
 [8] C. Weedbrook, S. Pirandola, R. Garcia-Patron, N. J. Cerf, T. C. Ralph, J. H. Shapiro, and S. Lloyd, Gaussian quantum information, *Reviews of Modern Physics* **84**, 621 (2012).
 [9] T. Heinosaari, A. S. Holevo, and M. M. Wolf, The semigroup structure of Gaussian channels, *Quantum Information and Computation* **10**, 619 (2010).
 [10] A. S. Holevo and V. Giovannetti, Quantum channels and their entropic characteristics, *Reports on Progress in Physics* **75**, 046001 (2012).
 [11] C. Gardiner and P. Zoller, *Quantum Noise* (Springer, 2004).
 [12] D. Petz, Sufficiency of channels over von Neumann algebras, *The Quarterly Journal of Mathematics* **39**, 97 (1988).
 [13] H. Kwon, R. Mukherjee, and M. S. Kim, Reversing Lindblad Dynamics via Continuous Petz Recovery Map, *Physical Review Letters* **128**, 020403 (2022).
 [14] A. J. Parzygnat and J. Fullwood, From Time-Reversal Symmetry to Quantum Bayes’ Rules, *PRX Quantum* **4**, 020334 (2023).
 [15] R. Nasu, G. Tanaka, and A. Tsuchiya, Quantum Reversibility Meets Classical Reverse Diffusion, arXiv:2510.18512 (2025).
 [16] D. Petz, Monotone metrics on matrix spaces, *Linear Algebra and its Applications* **244**, 81 (1996).
 [17] F. Toscano, D. S. Tasca, A. M. C. de Almeida, A. J. Roncaglia, T. O. Maciel, L. C. Celeri, and S. P. Walborn, Quantum de Bruijn identity for Gaussian dynamical semigroups, *Physical Review A* **104**, 062207 (2021).
 [18] H. Vahlbruch, M. Mehmet, K. Danzmann, and R. Schnabel, Detection of 15 dB squeezed states of light and their application for the absolute calibration of photoelectric quantum efficiency, *Physical Review Letters* **117**, 110801 (2016).
 [19] H. Barnum and E. Knill, Reversing quantum dynamics with near-optimal quantum and classical fidelity, *Journal of Mathematical Physics* **43**, 2097 (2002).
 [20] O. Fawzi and R. Renner, Quantum Conditional Mutual Information and Approximate Markov Chains, *Communications in Mathematical Physics* **340**, 575 (2015).
 [21] M. Junge, R. Renner, D. Sutter, M. M. Wilde, and A. Winter, Universal Recovery Maps and Approximate Sufficiency of Quantum Relative Entropy, *Annales Henri Poincaré* **19**, 2955 (2018).